The effects of CCR5 inhibition on regulatory T-cell recruitment to colorectal cancer

S T Ward[*,1], K K Li[2], E Hepburn[2], C J Weston[2], S M Curbishley[2], G M Reynolds[2], R K Hejmadi[3], R Bicknell[4], B Eksteen[5], T Ismail[3], A Rot[4] and D H Adams[2]

[1]Centre for Liver Research & NIHR Birmingham Biomedical Research Unit, Level 5 Institute for Biomedical Research, University of Birmingham, Vincent Drive, Birmingham B15 2TT, UK; [2]National Institute for Health Research (NIHR) Birmingham Liver Biomedical Research Unit (BRU), University of Birmingham, Vincent Drive, Birmingham B15 2TT, UK; [3]Queen Elizabeth Hospital Birmingham, Mindelsohn Way, Birmingham B15 2WW, UK; [4]Institute for Biomedical Research, University of Birmingham, Vincent Drive, Birmingham B15 2TT, UK and [5]Snyder Institute, University of Calgary, Alberta T2N 4N1, Canada

Background: Regulatory T cells (Treg) are enriched in human colorectal cancer (CRC) where they suppress anti-tumour immunity. The chemokine receptor CCR5 has been implicated in the recruitment of Treg from blood into CRC and tumour growth is delayed in CCR5 − / − mice, associated with reduced tumour Treg infiltration.

Methods: Tissue and blood samples were obtained from patients undergoing resection of CRC. Tumour-infiltrating lymphocytes were phenotyped for chemokine receptors using flow cytometry. The presence of tissue chemokines was assessed. Standard chemotaxis and suppression assays were performed and the effects of CCR5 blockade were tested in murine tumour models.

Results: Functional CCR5 was highly expressed by human CRC infiltrating Treg and CCR5^{high} Treg were more suppressive than their CCR5^{low} Treg counterparts. Human CRC-Treg were more proliferative and activated than other T cells suggesting that local proliferation could provide an alternative explanation for the observed tumour Treg enrichment. Pharmacological inhibition of CCR5 failed to reduce tumour Treg infiltration in murine tumour models although it did result in delayed tumour growth.

Conclusions: CCR5 inhibition does not mediate anti-tumour effects as a consequence of inhibiting Treg recruitment. Other mechanisms must be found to explain this effect. This has important implications for anti-CCR5 therapy in CRC.

Regulatory T cells (Treg) are enriched in CRC relative to other tissue compartments (Loddenkemper et al, 2006; Salama et al, 2009; Sinicrope et al, 2009). Tumour Treg enrichment occurs in cancer-bearing mouse models and anti-tumour immunity is promoted through Treg depletion in several models including CRC (Ha, 2009). This is the basis of the Treg-mediated tumour immune escape hypothesis. (Danke et al, 2004).

Two populations of Treg exist: naturally occurring (nTreg) are generated in the thymus (Darrasse-Jèze et al, 2005), whereas induced Treg (iTreg) differentiate from CD4^{+}CD25^{-} cells in the presence of TGF-ß (Fantini et al, 2004). Both nTreg and iTreg express the canonical Treg markers: CD25, Foxp3 and CTLA-4 and it is thus difficult to distinguish the two. Recently, the stability of nTreg Foxp3 expression has been linked to demethylation of CpG

motifs in a highly conserved element of the Foxp3 locus known as the Treg-specific determining region (TSDR) (Floess et al, 2007).

Treg recruitment to tumours from blood is regulated by their ability to cross tumour endothelium promoted by functional chemokine receptors and adhesion molecules (Adams and Eksteen, 2006). In human ovarian cancer, the tumour expresses CCL22 allowing it to recruit CCR4^{+} Treg (Curiel et al, 2004) and in gastric cancer, tumour Treg infiltration correlated with CCL17 + or CCL22 + cell infiltration (Mizukami et al, 2008). More recently, CCR5 and CCR6 have been implicated. In a murine model of pancreatic cancer, CCR5 expression was demonstrated on tumour-infiltrating Treg (Tan et al, 2009) and reduction of tumour CCL5 expression by shRNA was associated with smaller tumours and reduced tumour Treg infiltration. The same effect was

---

demonstrated for subcutaneous tumours originating from a CRC cell line (Chang *et al*, 2012). Furthermore, delayed tumour growth with an associated reduction in tumour Treg infiltration is reported in CCR5 − / − mice compared with wild-type mice (Chang *et al*, 2012; Schlecker *et al*, 2012).

Studies investigating the role of CCR5 in mouse models of human disease are hampered by the fact that no selective antagonist or neutralising antibody to murine CCR5 currently exists (Mansfield *et al*, 2009). In contrast, a human CCR5 small molecular antagonist, Maraviroc, has been approved for the treatment of patients with HIV infection, acting by inhibition of viral entry through the CCR5 receptor (Ray, 2009). The drug has an excellent safety profile, is highly selective for CCR5 and is administered orally (Dorr *et al*, 2005) leading to the potential of developing clinical trials in patients with CRC. Maraviroc possesses no activity, however, against murine CCR5 (Saita *et al*, 2007). This led us to study the role of CCR5 in Treg recruitment to CRC with the view to developing a clinical trial using Maraviroc in patients with CRC.

METHODS

Human samples. Peripheral blood and tissue samples of CRC, adjacent distal colon and tumour-draining lymph node (TDLN) were obtained from patients undergoing a bowel resection as part of their treatment for CRC at the QEHB. Peripheral blood was also obtained, with consent, from healthy volunteers. Ethical approval had been obtained from the local research and ethics committee (LREC South Birmingham 2003/242, renewed 2012) and all patients donating tissue had given full prior consent.

Lymphocyte isolation. Mechanical digestion of tissue samples was performed using the gentleMACS dissociator (Miltenyi Biotec Ltd, Surrey, UK), in order to avoid denaturation of cell-surface epitopes (Mulder *et al*, 1994; Ford *et al*, 1996; Diederichsen *et al*, 1999). Enzymatic digestion of tissues in collagenase II solution (20 mg ml^{-1}, C2-22, VWR International Ltd, Leicestershire, UK) for 1 h increases the lymphocyte yield (Grange *et al*, 2011) and was used to obtain lymphocytes for use in functional assays. Digested tissue was passed through a cell strainer (BD Biosciences Ltd, Oxford, UK) and layered on top of a discontinuous gradient of 70% and 30% Percoll solutions (GE Healthcare Ltd, Buckinghamshire, UK). The mononuclear cell band was aspirated and the cell suspension was washed and resuspended in complete media containing 1% foetal calf serum (FCS) and antibiotics (penicillin 1 U ml^{-1}, streptomycin 1 μg ml^{-1}, gentamicin 10 μg ml^{-1}, amphotericin B 0.25 μg ml^{-1}).

Lymphocyte phenotyping and cell sorting. The cell suspension was labelled with a fixable live/dead marker (Life Technologies Ltd, Paisley, UK) and the following antibodies: CD3-Alexa-Fluor 750 (Clone UCHT1, Abd Serotec, Oxford, UK), CD4-V500 (Clone RPA-T4, BD), CD8-PE-CF594 (Clone RPA-T8, BD), CD25 (Clone M-A251, BD) and CD127-FITC (Clone HIL-7R-M21, BD). Cells were labelled with additional antibodies against various cell-surface and intra-cellular markers. In certain experiments, cells were fixed and permeabilised using formalin and saponin solutions prior to intra-cellular antibody labelling. Samples were analysed using a CyAn ADP 3-laser, 9-colour flow cytometer (Beckman Coulter Inc, Brea, CA, USA). The Treg population was defined by gating on live CD3$^+$ CD4$^+$ CD25$^+$ CD127^{low} cells. Conventional T cells (Tconv) were defined by gating on live CD3$^+$ CD4$^+$ CD25$^-$ cells. To obtain purified Treg and Tconv for functional assays, antibody-labelled cells were sorted using a MoFlo XDP High-Speed Cell Sorter (Beckman Coulter Inc) in purity mode.

Suppression assay. Responder T cells (Tresp) were obtained by isolating lymphocytes from 10 ml of peripheral blood from an unmatched donor and labelling with CellTrace Violet dye (Life Technologies Ltd). An equal number of CCR5^{low} Treg, CCR5^{high} Treg and Tconv were three-way sorted into a round-bottomed 96-well plate. Violet-labelled Tresp were then plate-sorted into the same wells yielding Treg:Tresp ratios of 1 : 1, 1 : 2 or 1 : 4. Human Treg Suppression Inspector beads (Miltenyi Biotec Ltd) provided a polyclonal stimulus for proliferation and were added to each well at a bead:lymphocyte ratio of 1 : 2. The total volume of each well was made up to 200 μl with RPMI + 10% FCS. The plate was incubated at 37 °C and 5% CO$_2$ for 3 days. Violet dye wash-out was analysed by flow cytometry. Results were reported as percent suppression (McMurchy and Levings, 2012):

$$\text{Percent suppression} = 100 - \frac{\text{Percentage of proliferating cells with Treg present}}{\text{Percentage of proliferating cells without Treg present}} \times 100$$

Transwell cell migration assay. Bead-free CD3$^+$ cells were purified from CRC cell suspension by positive immunomagnetic selection (Dynabeads FlowComp Human CD3, Life Technologies Ltd). Purity was > 95%. Cells were washed and suspended in RPMI + 0.1% bovine serum albumin (BSA) and incubated overnight with either 1 μM Maraviroc or an equal volume of DMSO vehicle, prior to the transwell assay. In the bottom of a 96-well transwell plate (Corning Inc, Corning, NY, USA), RPMI + 0.1% BSA either alone or containing 20 ng ml^{-1} recombinant CCL4 (Peprotech Inc, Rocky Hill, NJ, USA) was placed. CD3$^+$ cell suspension was placed in the upper compartment of the transwell and the plate was incubated at 37 °C 5% CO$_2$ for 4 h. Migrated and non-migrated cells were harvested, labelled with antibodies against CD4, CD25 and CD127, and analysed using the CyAn flow cytometer after addition of 20 μl AccuCheck counting beads (Life Technologies Ltd). The chemotactic index for the absolute number or percentage of a lymphocyte subset was reported:

$$\text{Chemotactic index} = \frac{\text{The absolute number (or percentage) of a lymphocyte subset that migrated in response to chemokine}}{\text{The absolute number (or percentage) of the subset that migrated to media alone}}$$

Immunohistochemistry. Formalin-fixed paraffin-embedded (FFPE) 5 μm sections were deparaffinised and rehydrated by passage through Clearene (Leica GmBH, Wetzlar, Germany) and graduated alcohols. Antigen retrieval was via microwaving in pre-heated EDTA buffer (0.37 g EDTA in 1 l distilled water, pH adjusted to 8.0 using 1N sodium hydroxide, 0.05% Tween 20) for 15 min. Frozen 5 μm sections were thawed and fixed in acetone for 5 min. Endogenous peroxidase was blocked by incubation with Perox-idase-Blocking Solution (Dako Ltd, Cambridge, UK) for 10 min. Fc receptors were blocked by incubation in 10% casein solution (Vector Labs Inc, Burlingame, CA, USA) for 30 min. Sections were incubated in a primary antibody solution to the target antigen at a pre-determined dilution (goat polyclonal anti-CCL3, anti-CCL4, anti-CCL5, anti-CCL20, all at 10 μg/ml, R&D Systems, Abingdon, UK) or an isotype-matched control antibody solution at equal concentration for 1 h at room temperature. The sections were incubated in an HRP-conjugated development solution (Vector ImmPress, Vector Labs Inc) and visualised in either ImmPACT NovaRED or ImmPACT DAB-Nickel (Vector Labs Inc). Sections were counter-stained in Meyer's haematoxylin (Dako Ltd), cleared and mounted in DPX (Leica GmBH). Tissue expression was visualised using a Leica DM6000 microscope and the manufac-turer's software.

For double immunohistochemistry, following antigen visualisa-tion with DAB-Nickel (anti-Foxp3, Clone 236A/E7, 10 μg ml^{-1}, Abcam, Cambridge, UK), sections were re-blocked with casein solution then incubated with the second primary antibody solution (anti-CCR5, Clone 45531, 10 μg ml^{-1}, R&D Systems Inc) for 1 h at

room temperature. Sections were incubated with the Vector ImmPress system as before, visualised with NovaRED.

Real-time PCR. RNA was extracted from snap-frozen tissue samples using the Qiagen RNeasy minikit (Qiagen GmBH, Hilden, Germany) and the concentration was adjusted to $100 \mu g \, ml^{-1}$ following assessment of RNA quantity by UV absorbance at 260/280 nm. Three micrograms of RNA was reverse-transcribed using the iScript kit (Bio-Rad Inc, Hercules, CA, USA). Differences in chemokine mRNA expression between CRC and matched colon tissue was assessed in duplicate, relative to chosen housekeeping genes, calculated by the $2(-\Delta\Delta Ct)$ method.

RNA was isolated from CRC-sorted Treg and Tconv using the RNeasy micro kit (Qiagen GmBH) and transcribed into cDNA (iScript). Gene expression was compared between Treg and Tconv relative to GAPDH. All target primers and probes were pre-designed and obtained from Life Technologies.

Methylation at the Foxp3 locus. A total of 10 000 to 20 000 CCR5^{low} Treg, CCR5^{high} Treg and Tconv were cell-sorted from three different CRC samples and DNA was extracted using the DNeasy Blood & Tissue kit (Qiagen GmBH). DNA was bisulfite-treated (Epitect Bisulfite kit, Qiagen GmBH). The primers and probes used to amplify the TSDR region and detect allelic methylation status have been published previously (Tatura *et al*, 2012).

Western blotting. Protein was extracted from 30 mg snap-frozen tissue by incubation in ice-cold lysis buffer (CellLytic MT, Sigma-Aldrich Ltd, Dorset, UK) containing Proteinase Inhibitor Cocktail (Roche Ltd, Welwyn Garden City, UK). The lysate protein concentrations were determined against a BSA standard using a bicinchoninic acid (BCA) assay and normalised to 2 mg BSA per ml. Forty micrograms of protein per sample in SDS sample buffer containing 10 mM ß-mercaptoethanol and 8 M urea was resolved on a 12% SDS–PAGE gel and transferred to a nitrocellulose membrane. Membranes were blocked in 5% non-fat milk dissolved in PBS for 1 h at room temperature. Membranes were subsequently incubated overnight at 4 °C with goat anti-human antibodies against various chemokines or GUS (R&D Systems) followed by a 1 h room temperature incubation with HRP-conjugated anti-goat antibodies. Protein bands were detected with the PicoWest ECL system (Thermo Fisher Scientific Inc, Rockford, IL, USA). Membranes were not stripped.

Mice, tumour cell lines and CCR5 inhibitors. Procedures involving mice and their welfare were conducted in accordance with institutional guidelines that comply with United Kingdom national policies (Animals (Scientific Procedures) Act 1986). All animal experiments underwent rigorous scientific and ethical review by the Joint Ethics and Research Governance Committee of the University of Birmingham, UK. BALB/c wild-type mice were purchased from Charles River, Margate, UK. hCCR5KI mice, in which murine CCR5 is replaced by human CCR5 allowing the testing of human CCR5 inhibitors (Mansfield *et al*, 2009), were a gift from Pfizer Inc, New York, NY, USA and were bred to homozygosity. CT26 cells, an undifferentiated colon carcinoma cell line, and B16-F10 cells, a melanoma cell line, were purchased from the ATCC via LGC Standards, Teddington, UK. Both cell lines were transduced to express luciferase. Met-RANTES was a gift from Dr Amanda Proudfoot, Merck-Serono, Lucerne, Switzerland. TAK-779 (Repository reference: ARP968) was obtained from the Centre for AIDS Reagents, NIBSC and was donated by the AIDS Research and Reference Programme, Division of AIDS, NIAID, NIH. UK-484900 and Maraviroc were gifted by Pfizer Inc. A twice-daily dosing regime of UK-484900 results in complete functional CCR5 blockade and human CCR5 is activated by murine chemokines with the same EC_{50} as for human chemokines (Dorr, 2008).

Tumour cell *in vitro* proliferation assays. A total of 1×10^4 CT26 or B16-F10 cells were seeded into a 96-well plate in 200 μl of DMEM + 10% FCS. Met-RANTES, TAK-779, UK-484900 and PBS were added to wells at different concentrations in triplicate. The cells were cultured for 24 h at 37 °C 5% CO_2 until 40%–50% confluence. 20 μl of CellTiter 96 Aqueous One Solution (G3580, Promega Inc, Madison, WI, USA), an MTT reagent, was added to each well, incubated at 37 °C for 3 h and absorbance read at 490 nm.

Subcutaneous tumour models. A total of 5×10^5 CT26 cells or 2.5×10^5 B16-F10 cells were inoculated into the left flank of female BALB/c or hCCR5KI mice, respectively. Tumour engraftment was confirmed by bioluminescent imaging (BLI) at day 7 and further imaging was performed every 72 h thereafter. Once daily injection of met-RANTES and TAK-779 was commenced at day 7, or from day 0 in the case of UK-484900. Mice were culled at 10 days post commencement of treatment, following cardiac puncture and tumour and spleen tissue was harvested. Fresh tissue was analysed by flow cytometry and the proportion of live CD4^{+} cells that had a Treg phenotype (CD4^{+} Foxp3^{+}) was analysed.

RESULTS

Treg are enriched in human CRC. Lymphocytes were isolated from a total of 70 samples of CRC from 70 patients, with matched distal colon in 60 cases, matched TDLN in 8 cases and matched peripheral blood in 7 cases. The proportion of CD4^{+} cells that had a Treg phenotype (CD4^{+}CD25^{+}CD127^{low}), referred to as the *Treg proportion*, was calculated for each sample and compared across tissue compartments. There was no significant difference in the median Treg proportion in peripheral blood samples between healthy volunteers and CRC patients (2.6 IQR: 2.2–3.2 *vs* 3.7 IQR: 3.0–3.7, $P = 0.49$, Mann-Whitney). Differences in the Treg proportion between all other tissue compartments reached statistical significance (Distal colon 4.8 IQR: 3.0–6.3 *vs* CRC 14.2 IQR: 9.8–18.9 *vs* TDLN 9.1 IQR: 7.4–11). The absolute number of Treg, adjusted per mg of tissue, was 75 for CRC (IQR: 58–120) *vs* 7.7 for colon (IQR: 4.8–9.7), $P = 0.016$, Wilcoxon signed-rank test.

The median percentage Foxp3 expression was 93.5% (IQR: 92.0–96.2), 16.2% (IQR: 13.8–19.5) and 6.5% (IQR: 4.7–12.7) for CRC-isolated Treg, Tconv and CD8^{+} cells, respectively. The difference in Foxp3 expression between Treg and Tconv was statistically significant ($P < 0.01$, Wilcoxon-signed rank).

Factors associated with the CRC Treg proportion. Patient factors (age at operation, gender, mortality, local and distant recurrence) and CRC factors (position, grade, stage, extramural vascular invasion, tumour volume, MSI status) were tested for association with the tumour Treg proportion, measured in 70 separate CRC samples. There was no significant association between the tumour Treg proportion and any of these factors.

Treg express different chemokine receptors compared with conventional T cells. The expression of different chemokine receptors, integrins and various Treg markers was compared by flow cytometry between CRC-isolated Treg and CRC-isolated Tconv and CD8^{+} cells. Both differences in percentage expression and MFI were compared. The expression of the same markers was then compared between CRC-isolated Treg and Treg isolated from other compartments. Positive expression was defined relative to a FMO control containing an IMC of the same isotype as the antibody against the antigen of interest. Summary of data from 64 separate flow cytometry experiments is presented in the Supplementary Tables. Statistical significance was assessed by Wilcoxon ranked-sign test, adjusted for multiple comparisons using the Bonferroni method. CCR4 and CCR5 were significantly overexpressed by CRC-isolated Treg compared with Tconv, both

by percentage expression and MFI. Significantly, more CRC-isolated Treg expressed CCR5 compared with Treg isolated from distal colon. Representative flow cytometry data are shown in Figure 1A. The mean fold change in Foxp3 mRNA expression by cell-sorted CRC Treg relative to Tconv was 6.5 (s.d. = 3.1), serving as an internal control for expected differences in gene expression between the two cell types. The mean fold change in CCR5 mRNA expression was 2.6 (s.d. = 1.0), suggesting that the increased cell-surface expression of CCR5 by Treg compared with Tconv may, at least in part, be explained by greater CCR5 gene expression (see Figure 1B). Transcription factors involved in the regulation of CCR5 transcription, KLF2 and CREB1 were also significantly upregulated by Treg compared with Tconv. Double immunohistochemistry identified cells within the tumour stroma, expressing both CCR5 and Foxp3 (see Figure 1C).

CCR5 ligands are expressed by human CRC. The mRNA expression of a panel of 10 housekeeping genes was measured in eight samples of CRC with matched distal colon, of standardised RNA concentration, by absolute quantification real-time PCR. IPO8 and GUS were found to be the most stable housekeeping genes by GeNORM and Bestkeeper algorithms (data not shown).

The gene expression of cognate chemokines to receptors of interest were profiled in CRC and matched distal colon, relative to IPO8 and GUS. There was no significant difference in the expression of CCR4 ligands (CCL17, CCL22), CCR7 ligands (CCL19, CCL21), CXCR3 ligands (CXCL9, CXCL10, CXCL11) or the CCR6 ligand (CCL20). CCL3 and CCL4, but not CCL5, were significantly overexpressed by CRC compared with distal colon (see Figure 2A). These findings were corroborated at the protein level by both western blotting and ELISA (Mix-N-Match ELISArray Kit 336111, Qiagen GmBH) using tissue protein lysates (see Figure 2B and C). The ELISArray kit gives absorbance as the readout because no standard curves are generated. However, the absorbances lie on the linear part of the standard curve provided the values are between the negative and positive control values, as was the case for all samples. Immunohistochemistry of CRC sections for CCL3, CCL4 and CCL5 all showed staining in the epithelial cell cytoplasm and within the stroma. Additionally, CCL4 staining was noted on the endothelium (see Figure 2D).

CCL4 correlates with Foxp3 and Treg CCR5 expression. Exposure to cognate chemokine leads to CCR5 internalisation (Mueller and Strange, 2004). It may therefore be expected that CCR5$^+$ cells
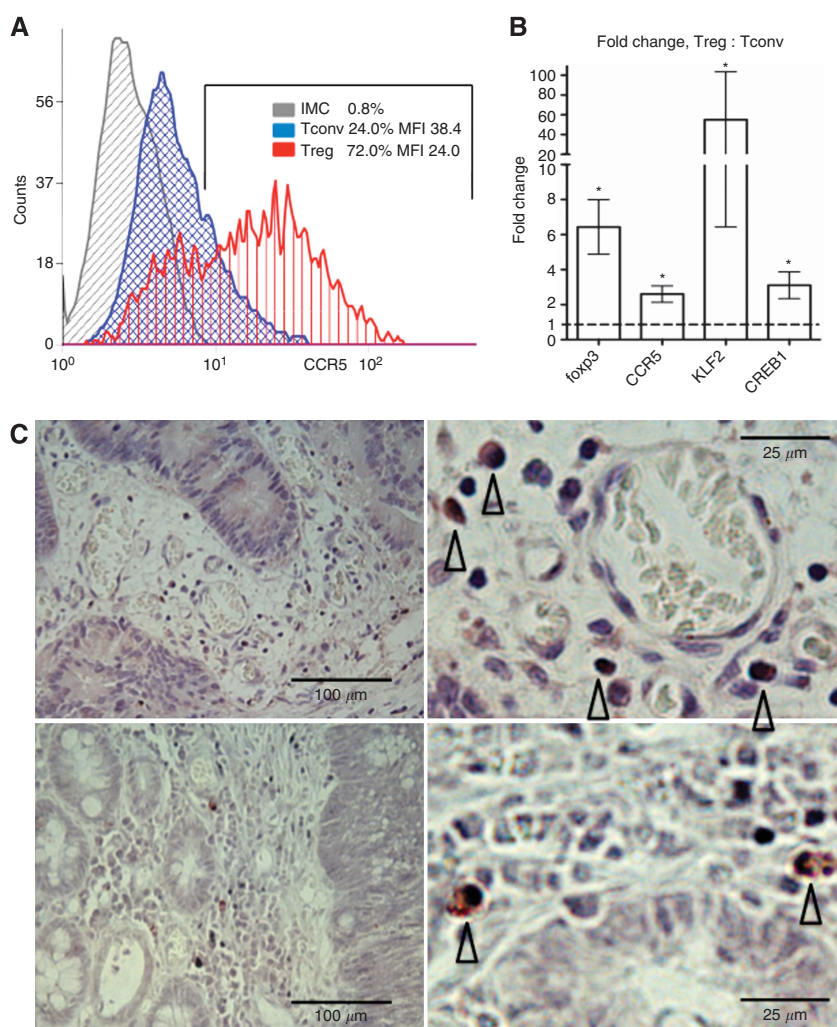

Figure 1. (**A**) Representative flow cytometry data of surface CCR5 expression by Tconv (blue) and Treg (red), isolated from CRC, compared with isotype-matched control antibody (grey, IMC). (**B**) Mean fold change in relative quantification of mRNA expression of Foxp3, CCR5, KLF2 and CREB1 to GAPDH by Treg relative to Tconv, isolated from CRC (n = 5). Error bars represent the standard error of the mean. Asterisks indicate statistically significant differences (Wilcoxon signed-rank test). (**C**) Double immunohistochemistry of FFPE CRC sections, stained for Foxp3 (black nuclear stain) and CCR5 (red cytoplasmic stain). Two representative samples are shown (top and bottom) of 4 samples stained. Two magnifications are shown (left, magnification × 100 and right, magnification × 400) (left, magnification × 100) and at higher magnification (right, × 400). Open arrows indicate double-positively stained cells. Abbreviation: CRC = colorectal cancer; FFPE = formalin-fixed paraffin-embedded.
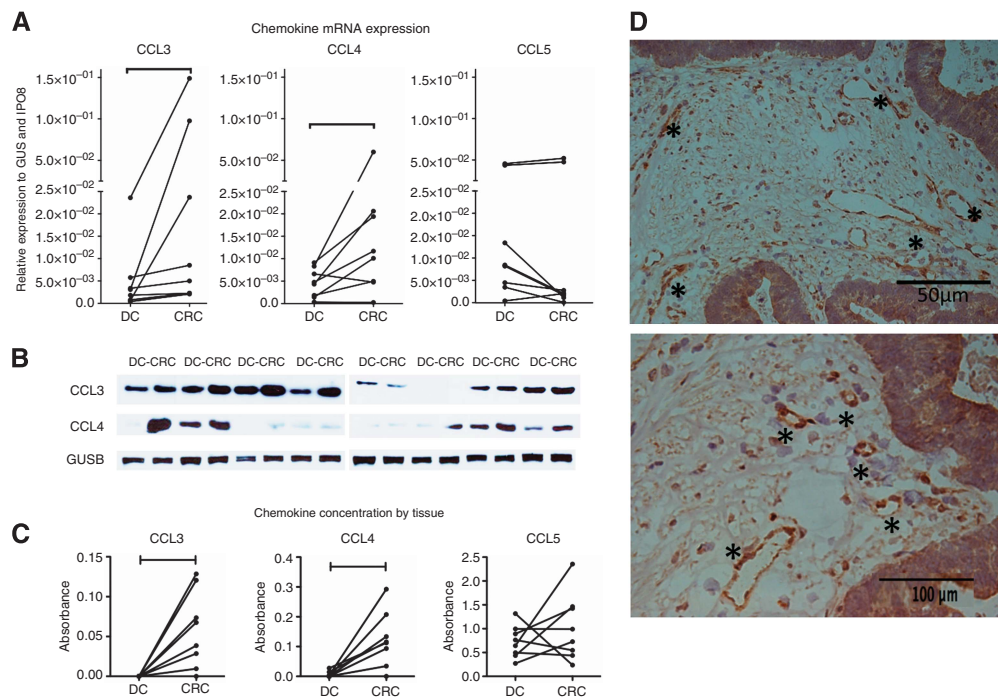
Figure 2. (**A**) Relative quantification of chemokine mRNA expression to GUS and IPO8 by tissue type. Capped lines indicate statistically significant differences (Wilcoxon signed-rank test). (**B**) Western blots probing for CCL3, CCL4 and GUS in eight samples of CRC with matched distal colon of standard protein concentration (2 mg BSA per ml). (**C**) Semi-quantitative measurement of CCL3, CCL4 and CCL5 levels by ELISA in eight samples of CRC with matched distal colon of standard protein concentration (2 mg BSA per ml). Capped lines indicate statistically significant differences (Wilcoxon signed-rank test). (**D**) Immunohistochemistry of CCL4 in frozen sections of CRC (representative of four cases), magnification $\times 200$ (top) and $\times 400$ (bottom). Asterisks indicate positive CCL4 staining of the tumour endothelium. Abbreviations: CRC = colorectal cancer; GUS = ß-glucuronidase; IPO8 = Importin-8; DC = distal colon; BSA = bovine serum albumin.

would internalise CCR5 after migration along a chemokine concentration gradient. CRC CCL3 and CCL4 mRNA expression correlated with CRC-Treg CCR5 expression (CCL3: $n = 12$, $r^2 = 0.61$, $P = 0.036$; CCL4: $n = 12$; $r^2 = 0.8$, $P = 0.002$). There was no correlation between CRC CCL3, CCL4 and CCL5 mRNA expression and the tumour Treg proportion although there was a significant correlation between CRC CCL4 mRNA and Foxp3 mRNA ($n = 18$, $r^2 = 0.61$, $P = 0.0078$). These correlations support the notion that CCR5 + Treg are recruited to CRC via cognate chemokines, particularly CCL3 and CCL4.

CRC-isolated Treg are nTreg. We studied Helios expression and unmethylated DNA at the TSDR in the CRC Treg because both had been associated with natural Treg. Median (IQR) percentage Helios expression by CRC-isolated Treg was 75.2% (70.6–80.8) compared with 11.2% (9.2–14.9) for Tconv ($P = 0.04$). DNA was extracted from cell-sorted CRC-isolated CCR5^{high} Treg, CCR5^{low} Treg and Tconv and TSDR analysis confirmed significantly more CCR5- and CCR5 + Treg had unmethylated DNA at the TSDR compared with Tconv ($P = 0.018$), see Figure 3A.

CCR5^{high} Treg are more suppressive than CCR5^{low} Treg. There was a trend for increased expression of Foxp3, CTLA-4 and CD39 by CRC-isolated CCR5^{high} Treg compared with CCR5^{low} Treg, although these differences did not reach statistical significance (data not shown). CRC-isolated Treg suppressed allogeneic T-cell proliferation whereas CRC-isolated Tconv did not (see Figure 3B), and CCR5^{high} Treg were more potent *in vitro* than CCR5^{low} Treg ($P = 0.018$).

CRC-isolated Treg migrate towards CCL4 *in vitro*. CRC-isolated lymphocytes were allowed to migrate towards $20\,ng\,ml^{-1}$ CCL4 across a transwell membrane, over five separate experiments. The mean proportion of isolated Treg that migrated across the transwell was 21% and 28% in response to media alone and CCL4, respectively ($P = 0.043$). The difference in the chemotactic

index between Treg migrating in response to CCL4 and in response to media alone reaching statistical significance ($P = 0.043$). Pre-treatment of lymphocytes with Maraviroc abolished the migration ($P = 0.042$). There was a reciprocal, significant reduction in the chemotactic index of the number of Treg remaining in the upper INPUT chamber with CCL4 compared with media alone ($P = 0.028$) (see Figure 3C). The Treg proportion of migrated cells was significantly increased in response to chemokine compared with media alone, $P = 0.043$ (see Figure 3D).

Treg exhibit enhanced proliferation compared with Tconv *in vivo*. Although tumour-isolated Treg did not proliferate *in vitro* (data not shown) as has been reported by others (Ling *et al*, 2007; Chaput *et al*, 2009), they expressed higher levels of the proliferation marker, Ki67, compared with Tconv, suggesting that they are highly proliferative *in vivo* (42% IQR: 20–63 *vs* 7.0% IQR: 3.6–15, $P = 0.032$).

CCR5 inhibition does not reduce Treg infiltration in murine tumour models. The above findings implicate CCR5 in Treg recruitment and function in human CRC and support the hypothesis that inhibiting CCR5 will reduce Treg function in CRC thereby enhancing anti-tumour immunity. We therefore sought to test this hypothesis by inhibiting CCR5 in murine tumour models. *In vitro* proliferation of CT26 and B16-F10 cells were not affected by increasing doses of met-RANTES and UK-484900 (see Figure 4A). However, TAK-779 significantly inhibited CT26 proliferation, consistent with a previous study demonstrating TAK-779-induced CT26 cytotoxicity (Cambien *et al*, 2011). CT26 and B16-F10 tumours were grown in BALB/c and hCCR5KI mice, respectively. Tumour Treg in both of these mice expressed significantly more CCR5 than Tconv and in the case of B16-F10 tumours, Treg expressed significantly more CCR5 than CD8$^+$ cells (see Figure 4B).
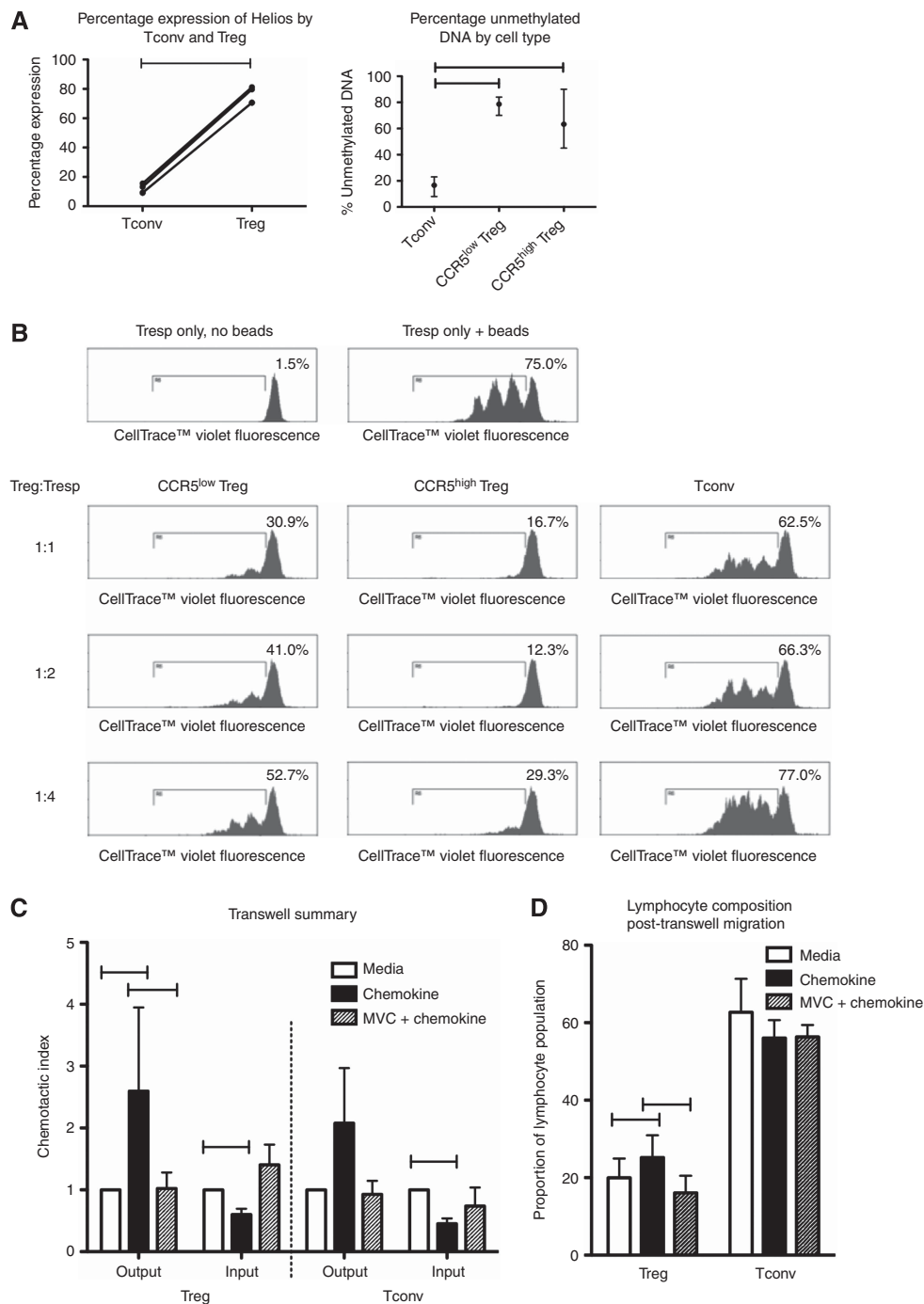
Figure 3. (A) Left: percentage expression of HELIOS by CRC-isolated Tconv and matched Treg, measured by flow cytometry ($n = 4$). Right: mean percentage methylation of the TSDR locus by cell type. Error bars represent the data range ($n = 4$). Capped lines indicate statistically significant differences (Mann–Whitney test). (B) Representative data from a Treg suppression assay: peripheral blood responder T cells (Tresp) were cultured alone (top left) or with Treg Suppression Inspector beads (Miltenyi Biotec Ltd, UK) (top right). Tresp were then cultured with CRC-isolated CCR5^{low} Treg, CCR5^{high} Treg or CD4$^+$CD25$^-$ (Tconv) cells at given ratios. Percentage in top right of each histogram represents the percentage proliferation of Tresp. (C) Transwell migration assay of CRC-isolated Treg (left) and Tconv (right), pre-treated with either 1 μM Maraviroc or DMSO-vehicle, to media alone or media containing 20 ng ml^{-1} recombinant CCL4 ($n = 6$ per group). (D) The Treg and Tconv fraction of lymphocytes migrating across the transwell. Capped lines indicate statistically significant differences between groups (Wilcoxon signed-rank test). Abbreviations: CRC = colorectal cancer; DMSO = dimethyl sulphoxide.

CCR5 inhibition via met-RANTES and TAK-779 in BALB/c mice or UK-484900 in hCCR5KI mice led to delayed tumour growth at multiple time-points, by BLI and calliper measurements (see Figure 5). The mean tumour weight was significantly less for all treatments compared with control injections (see Figure 5C and F). There was no difference in the tumour Treg proportion for any of the drug treatments compared with control injections (see Figure 6A and B). There was a trend for increased CCR5 ligand levels in the tumours of UK-484900-treated hCCR5KI mice compared with controls, this difference reaching statistical significance in the case of CCL5. There was also a trend for reduced tumour and tissue VEGF levels in UK-484900-treated hCCR5KI mice compared with controls (see Figure 6C).
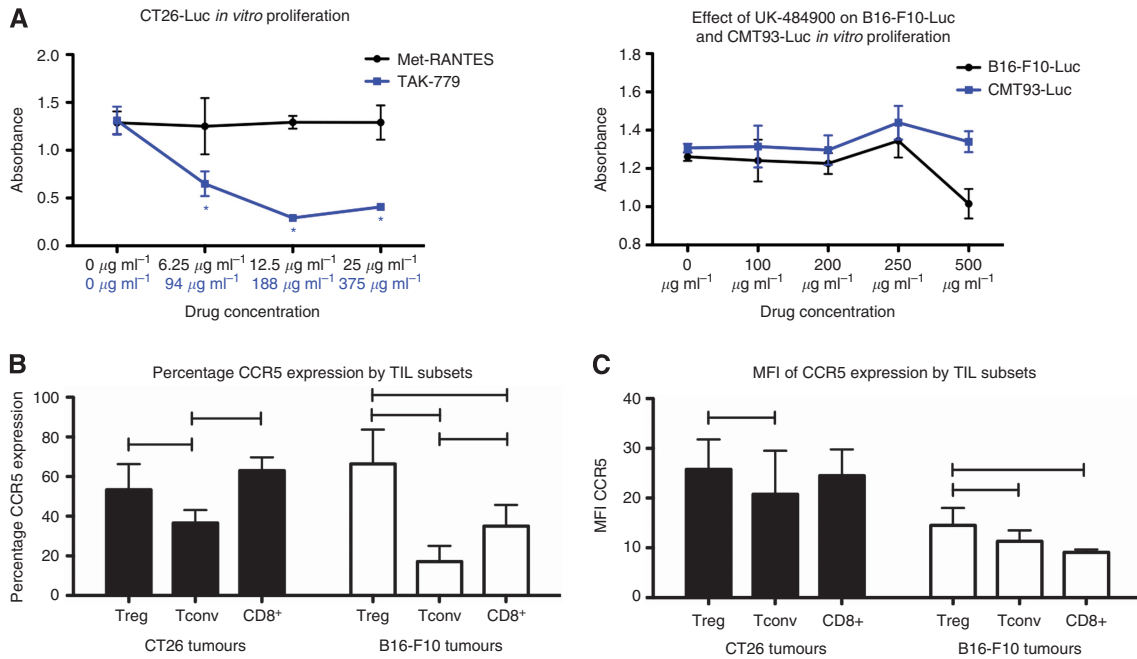
Figure 4. (**A**) *In vitro* proliferation assay of CT26 and B16-F10 cells cultured with different concentrations of met-RANTES (CT26), TAK-779 (CT26) and UK-484900 (B16-F10) in triplicate. Error bars represent 95% confidence intervals about the mean. (**B**, **C**) Median percentage and MFI expression of surface CCR5 by tumour-isolated Treg (CD4$^+$Foxp3$^+$), Tconv (CD4$^+$Foxp3$^-$) and CD8$^+$ cells, from wild-type BALB/c mice (CT26 tumours) and hCCR5KI mice (B16-F10 tumours) treated with 10 days of PBS ($n = 10$ per group). Error bars represent the IQR about the median. Capped lines indicate statistically significant differences (Wilcoxon signed rank test). Abbreviations: MFI = median fluorescent intensity; PBS = phosphate-buffered saline.
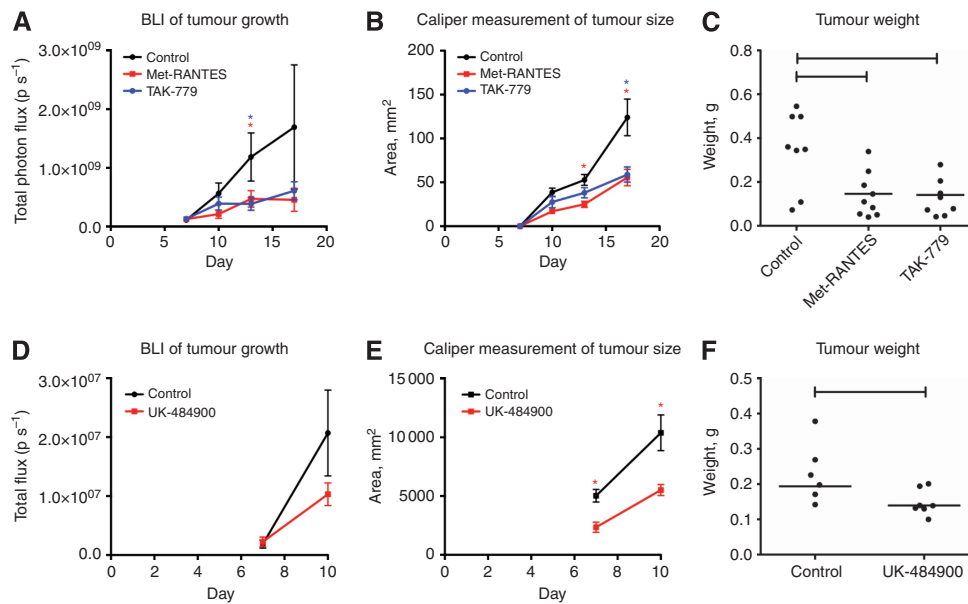

Figure 5. Tumour growth kinetics as measured by BLI for CT26 tumours in wild-type BALB/c mice (**A**) and B16-F10 tumours in hCCR5KI mice (**D**), treated with injections of PBS (controls) or CCR5 antagonists. Tumour growth kinetics by calliper measurements for CT26 tumours in wild-type BALB/c mice (**B**) and B16-F10 tumours in hCCR5KI mice (**E**), treated with injections of PBS (controls) or CCR5 antagonists. CT26 (**C**) and B16-F10 (**F**) tumour weights post resection in mice treated with PBS (controls) or CCR5 antagonists. Error bars represent the standard error about the mean. Asterisks indicate statistically significant differences compared with the control group (Mann–Whitney). Capped lines indicate statistically significant differences between groups (Mann–Whitney). Abbreviations: BLI = bioluminescent imaging; PBS = phosphate-buffered saline.

DISCUSSION

The Treg proportion was significantly increased in human CRC compared with distal colon, consistent with published data (Ling *et al*, 2007; Sinicrope *et al*, 2009; Frey *et al*, 2010; Yoon *et al*, 2012).

The reported association between tumour Treg enrichment and cancer stage in CRC is inconsistent. We calculated CRC-Treg infiltration as a proportion of CD4$^+$ cells by flow cytometry and found no demonstrable association between the Treg proportion and disease stage, findings that are consistent with previous studies taking the same approach (Deng *et al*, 2010). We found that
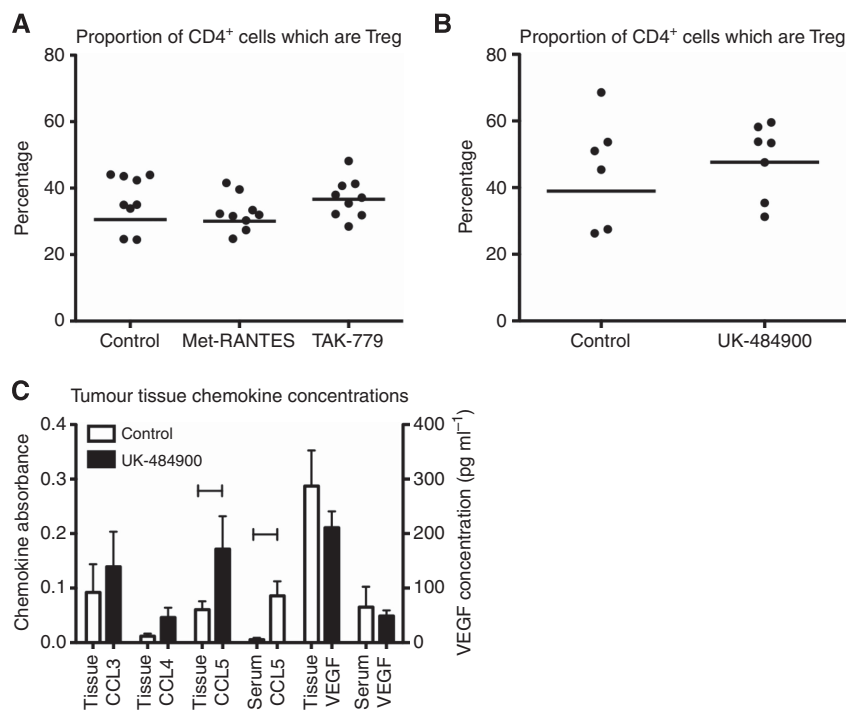
Figure 6. The proportion of tumour-isolated CD4$^+$ cells with a Treg (CD4$^+$Foxp3$^+$) phenotype, the *Treg proportion*, in BALB/c mice (**A**) and hCCR5KI mice (**B**), treated either with PBS (controls) or CCR5 antagonists. (**C**) Mean tumour tissue and serum levels of CCL3, CCL4, CCL5 and VEGF, measured by semi-quantitative ELISA, in hCCR5KI mice, treated either with PBS (controls) or UK-484900 ($n = 5$ per group). Error bars represent the standard error of the mean. Capped lines indicate statistically significant differences (Mann-Whitney). Abbreviations: hCCR5KI = human CCR5 knock-in; PBS = phosphate-buffered saline.

significantly more tumour-isolated Treg expressed CCR5 than Tconv and that levels of CCR5 were higher on the Treg than Tconv. Furthermore, Treg isolated from tumour expressed significantly more CCR5 than Treg isolated from distal colon. Two of the ligands for CCR5 (CCL3 and CCL4) were significantly overexpressed by CRC compared with distal colon, both at the mRNA and protein levels. CCL4 localised to the tumour endothelium, and CRC-ioslated Treg migrated to CCL4 *in vitro* suggesting that this chemokine may play a key role in the recruitment of CCR5$^+$ lymphocytes to the tumour. Several characteristics of the CRC-isolated T cells suggest they were nTreg including expression of Helios and had unmethylated DNA at the TSDR. We sorted CRC Treg based on levels of CCR5 expression and found that, CRC^{high} Treg were more potent suppressors of allogeneic T-cell proliferation *in vitro*, suggesting that CCR5 expression not only recruits Treg to the tumour but also defines a more potent suppressive function. These findings implicate CCR5 in Treg recruitment and function in human CRC and support the hypothesis that inhibiting CCR5 will reduce Treg function in CRC thereby enhancing anti-tumour immunity. To test this hypothesis we, used three different CCR5 antagonists to disrupt CCR5-dependent responses in murine models of CRC. Consistent with the findings from human CRC, Treg isolated from murine tumours expressed significantly more CCR5 than Tconv. CCR5 inhibition by RANTES, TAK-779 or UK 484900 resulted in a significant delay in tumour growth in two different CRC models. However, surprisingly, this was not associated with a reduction in tumour Treg infiltration compared with vehicle-treated mice. This suggests that Treg are not recruited to tumours, to any significant degree, via the CCR5 axis.

We did find that a significant proportion of Tconv and CD8$^+$ cells also expressed CCR5, albeit less so than Treg, and therefore the recruitment of all T cells may have been similarly inhibited. It is possible that CCR5 expression may be a marker for the expression of other receptors involved in the recruitment process or that Treg

are recruited by chemokine-independent mechanisms. Selective proliferation of Treg within the tumour tissue, enhanced Treg survival and reduced Treg egress could all explain Treg enrichment in CRC. Significantly more human CRC-Treg were proliferating, as demonstrated by Ki67 expression compared with Tconv consistent with findings in other cancer models (Gobert *et al*, 2009; Wainwright *et al*, 2011). Others have suggested that Treg may be induced *in situ* in tumours from other T cells (Liu *et al*, 2007), but our finding that tumour Treg TSDR locus was unmethylated makes this unlikely to be the sole mechanism for Treg enrichment in human CRC.

CCR5 expression is associated with T-cell activation and proliferation (Richardson *et al*, 2012; Wierda *et al*, 2012). The factors leading to the expression of surface CCR5 are complex and involve receptor internalisation, recycling and gene transcription (Tan *et al*, 2009; Chang *et al*, 2012; Schlecker *et al*, 2012). Greater surface CCR5 expression by Treg compared with Tconv may therefore represent differences in activation status rather than preferential recruitment via the CCR5 axis. In support of this, the gene expression of the transcription factors regulating CCR5 expression, KLF-2 and CREB-1, were significantly upregulated by CRC-isolated Treg compared with Tconv.

Several previous studies have reported that lines of evidence that CCR5 inhibition leads to a reduction in Treg infiltration in murine tumours. Firstly, CCL5 knockdown in tumour cell lines leads to delayed tumour growth with reduced Treg infiltration compared with wild-type cell lines (Tan *et al*, 2009; Chang *et al*, 2012). Secondly, tumour growth in CCR5 − / − mice is delayed with associated reduced Treg infiltration compared with wild-type mice (Chang *et al*, 2012; Schlecker *et al*, 2012). Thirdly, inhibition of CCR5 by TAK-779 reduces tumour Treg infiltration compared with vehicle control in a pancreatic cancer model (Tan *et al*, 2009). It was therefore surprising that pharmacological CCR5 inhibition did not lead to a detectable reduction in tumour Treg infiltration in our models. CCR5 inhibition did, however, lead to a delay in

tumour growth in keeping with previously published findings (Tan et al, 2009; Cambien et al, 2011; Chang et al, 2012).

How did CCR5 inhibition lead to a delay in tumour growth but no associated reduction in tumour Treg infiltration? CCR5 antagonism by met-RANTES and TAK-779 is not specific. It is possible that co-inhibition of CCR1 (met-RANTES) or CXCR3 (TAK-779) affected the recruitment of other T-cell subsets so that the Treg proportion effectively remained unchanged. However, this does not explain the delayed tumour growth observed in UK-484900-treated hCCR5KI mice. This drug does not affect tumour proliferation in vitro consistent with a specific antagonism of human and not murine CCR5. This suggests that anti-tumour activity is due to the effects on host CCR5 and thus mediated via immune cells and not a direct effect on tumour cells. Inhibition of CCR5 could reduce the migration of other cells into the tumour or lead to increased recruitment via other chemokine receptors. Inhibition of CCR5 by UK-484900 led to increased tumour and serum levels of CCL5, which could promote recruitment via CCR1 as has been shown for NK cells in a model of hepatitis (Ajuebor et al, 2007). There is a significant increase in $CD4^+$, $CD8^+$ and NK cell tissue infiltration and a decrease in macrophage tissue infiltration in CCR5 $-/-$ mice compared to wild-type mice (Kuziel et al, 2003; Song et al, 2012). Because macrophages can promote tumour growth, it is possible that the CCR5 effect is mediated via changes in macrophage recruitment. Such changes could delay tumour growth while having no effect on the Treg proportion. CCR5 also mediates recruitment of endothelial cells. Neovascularisation is inhibited in CCR5 $-/-$ mice compared with wild-type mice, associated with lower levels of tissue VEGF (Ambati et al, 2003; Ishida et al, 2012). Endothelial progenitor cells are recruited to tumours from the bone marrow in a CCR5-dependent manner, where they lead to the formation of neovessels (Spring et al, 2005). By reducing tumour neovessel formation through blockade of endothelial cell recruitment, CCR5 inhibition could delay tumour growth, independent of effects on Treg recruitment. In support of this, we observed a trend for lower levels of tumour and serum VEGF in UK-484900-treated mice although this did not reach significance.

A previous study reported reduced tumour Treg infiltration of pancreatic cancer in mice treated with TAK-779 (Tan et al, 2009). This is very different from our findings and could be due to a difference in the tumour models. In the pancreatic cancer paper, tumour Treg proportion in control mice was 74% compared with 49% in TAK-779-treated mice. This is a very high tumour Treg proportion in control mice and the reduction to 49% in treated mice is still higher than the tumour Treg proportion in control mice from other experiments.

Potential explanations for a low tumour Treg infiltration in CCR5 $-/-$ mice include: (i) Treg accumulate in the thymus in CCR5 $-/-$ mice, associated with a reduction in S1PR1 expression compared with wild-type mice (Kroetz and Deepe, 2011) resulting in a failure of egress; (ii) T cells from CCR5 $-/-$ mice secrete lower levels of IL-2 and NFAT following activation compared with T cells from wild-type mice (Camargo et al, 2009) and CCR5$^+$ T cells are more proliferative than their CCR5$^-$ counterparts. Accordingly, tumour-resident Treg in CCR5 $-/-$ mice may be relatively anergic. (iii) Lower VEGF levels have been reported in CCR5 $-/-$ mice compared to wild-type mice (Ambati et al, 2003; Ishida et al, 2012) and some Treg express the VEGF receptor and proliferate in response to VEGF (Terme et al, 2013).

In conclusion, although conditions in human CRC exist to support active recruitment of Treg via the CCR5 axis, pharmacological inhibition of CCR5 in murine tumour models fail to demonstrate any reduction in tumour Treg infiltration despite reducing tumour growth. This suggests that the effect of CCR5 antagonism in CRC is not through Treg depletion, but must involve other immune pathways. Caution should be exercised before moving into clinical trials of CCR5 inhibition in CRC.

CONFLICT OF INTEREST

The authors declare no conflict of interest.

REFERENCES

Adams DH, Eksteen B (2006) Aberrant homing of mucosal T cells and extra-intestinal manifestations of inflammatory bowel disease. Nat Rev Immunol 6: 244–251.

Ajuebor MN, Wondimu Z, Hogaboam CM, Le T, Proudfoot AEI, Swain MG (2007) CCR5 deficiency drives enhanced natural killer cell trafficking to and activation within the liver in murine T cell-mediated hepatitis. Am J Pathol 170: 1975–1988.

Ambati BK, Anand A, Joussen AM, Kuziel WA, Adamis AP, Ambati J (2003) Sustained inhibition of corneal neovascularization by genetic ablation of CCR5. Invest Ophthalmol Vis Sci 44: 590–593.

Camargo JF, Quinones MP, Mummidi S, Srinivas S, Gaitan AA, Begum K, Jimenez F, VanCompernolle S, Unutmaz D, Ahuja SS, Ahuja SK (2009) CCR5 expression levels influence NFAT translocation, IL-2 production, and subsequent signaling events during T lymphocyte activation. J Immunol 182: 171–182.

Cambien B, Richard-Fiardo P, Karimdjee BF, Martini V, Ferrua B, Pitard B, Schmid-Antomarchi H, Schmid-Alliana A (2011) CCL5 neutralization restricts cancer growth and potentiates the targeting of PDGFRβ in colorectal carcinoma. PLoS One 6: e28842.

Chang L-Y, Lin Y-C, Mahalingam J, Huang C-T, Chen T-W, Kang C-W, Peng H-M, Chu Y-Y, Chiang J-M, Dutta A, Day Y-J, Chen T-C, Yeh C-T, Lin C-Y (2012) Tumor-derived chemokine CCL5 enhances TGF-ß mediated killing of CD8 + T cells in colon cancer by T regulatory cells. Cancer Res 72: 1092–1102.

Chaput N, Louafi S, Bardier A, Charlotte F, Vaillant J-C, Ménégaux F, Rosenzwajg M, Lemoine F, Klatzmann D, Taieb J (2009) Identification of CD8 + CD25 + Foxp3 + suppressive T cells in colorectal cancer tissue. Gut 58: 520–529.

Curiel TJ, Coukos G, Zou L, Alvarez X, Cheng P, Mottram P, Evdemon-Hogan M, Conejo-Garcia JR, Zhang L, Burow M, Zhu Y, Wei S, Kryczek I, Daniel B, Gordon A, Myers L, Lackner A, Disis ML, Knutson KL, Chen L, Zou W (2004) Specific recruitment of regulatory T cells in ovarian carcinoma fosters immune privilege and predicts reduced survival. Nat Med 10: 942–949.

Danke NA, Koelle DM, Yee C, Beheray S, Kwok WW (2004) Autoreactive T cells in healthy individuals. J Immunol 172: 5967–5972.

Darrasse-Jèze G, Marodon G, Salomon BL, Catala M, Klatzmann D (2005) Ontogeny of CD4 + CD25 + regulatory/suppressor T cells in human fetuses. Blood 105: 4715–4721.

Deng L, Zhang H, Luan Y, Zhang J, Xing Q, Dong S, Wu X, Liu M, Wang S (2010) Accumulation of Foxp3 + T regulatory cells in draining lymph nodes correlates with disease progression and immune suppression in colorectal cancer patients. Clin Cancer Res 16: 4105–4112.

Diederichsen ACP, Zeuthen J, Christensen PB, Kristensen T (1999) Characterisation of tumour infiltrating lymphocytes and correlations with immunological surface molecules in colorectal cancer. *Eur J Cancer* **35**: 721–726.

Dorr P (2008) Maraviroc outlook in HIV and non-HIV diseases. *HIV infection and organ transplantation symposium.* University Medical Center Hamburg-Eppendorf: Hamburg, Germany.

Dorr P, Westby M, Dobbs S, Griffin P, Irvine B, Macartney M, Mori J, Rickett G, Smith-Burchnell C, Napier C, Webster R, Armour D, Price D, Stammen B, Wood A, Perros M (2005) Maraviroc (UK-427,857), a potent, orally bioavailable, and selective small-molecule inhibitor of chemokine receptor CCR5 with broad-spectrum anti-human immunodeficiency virus type 1 activity. *Antimicrob Agents Chemother* **49**: 4721–4732.

Fantini MC, Becker C, Monteleone G, Pallone F, Galle PR, Neurath MF (2004) Cutting edge: TGF-beta induces a regulatory phenotype in CD4 + CD25- T cells through Foxp3 induction and down-regulation of Smad7. *J Immunol* **172**: 5149–5153.

Floess S, Freyer J, Siewert C, Baron U, Olek S, Polansky J, Schlawe K, Chang H-D, Bopp T, Schmitt E, Klein-Hessling S, Serfling E, Hamann A, Huehn J (2007) Epigenetic control of the foxp3 locus in regulatory T cells. *PLoS Biol* **5**: e38.

Ford AL, Foulcher E, Goodsall AL, Sedgwick JD (1996) Tissue digestion with dispase substantially reduces lymphocyte and macrophage cell-surface antigen expression. *J Immunol Methods* **194**: 71–75.

Frey DM, Droeser RA, Viehl CT, Zlobec I, Lugli A, Zingg U, Oertli D, Kettelhack C, Terracciano L, Tornillo L (2010) High frequency of tumor-infiltrating FOXP3 regulatory T cells predicts improved survival in mismatch repair-proficient colorectal cancer patients. *Int J Cancer* **126**: 2635–2643.

Gobert M, Treilleux I, Bendriss-Vermare N, Bachelot T, Goddard-Leon S, Arfi V, Biota C, Doffin AC, Durand I, Olive D, Perez S, Pasqual N, Faure C, Ray-Coquard I, Puisieux A, Caux C, Blay J-Y, Ménétrier-Caux C (2009) Regulatory T Cells recruited through CCL22/CCR4 are selectively activated in lymphoid infiltrates surrounding primary breast tumors and lead to an adverse clinical outcome. *Cancer Res* **69**: 2000–2009.

Grange C, Létourneau J, Forget M-A, Godin-Ethier J, Martin J, Liberman M, Latour M, Widmer H, Lattouf J-B, Piccirillo CA, Cailhier J-F, Lapointe R (2011) Phenotypic characterization and functional analysis of human tumor immune infiltration after mechanical and enzymatic disaggregation. *J Immunol Methods* **372**: 119–126.

Ha T-Y (2009) The role of regulatory T cells in cancer. *Immune Netw* **9**: 209.

Ishida Y, Kimura A, Kuninaka Y, Inui M, Matsushima K, Mukaida N, Kondo T (2012) Pivotal role of the CCL5/CCR5 interaction for recruitment of endothelial progenitor cells in mouse wound healing. *J Clin Invest* **122**: 711–721.

Kroetz DN, Deepe GS (2011) An aberrant thymus in CCR5(-/-) mice is coupled with an enhanced adaptive immune response in fungal infection. *J Immunol* **186**: 5949–5955.

Kuziel WA, Dawson TC, Quinones M, Garavito E, Chenaux G, Ahuja SS, Reddick RL, Maeda N (2003) CCR5 deficiency is not protective in the early stages of atherogenesis in apoE knockout mice. *Atherosclerosis* **167**: 25–32.

Ling KL, Pratap SE, Bates GJ, Singh B, Mortensen NJ, George BD, Warren BF, Piris J, Roncador G, Fox SB, Banham AH, Cerundolo V (2007) Increased frequency of regulatory T cells in peripheral blood and tumour infiltrating lymphocytes in colorectal cancer patients. *Cancer Immun* **7**: 7.

Liu VC, Wong LY, Jang T, Shah AH, Park I, Yang X, Zhang Q, Lonning S, Teicher BA, Lee C (2007) Tumor evasion of the immune system by converting CD4 + CD25- T cells into CD4 + CD25 + T regulatory cells: role of tumor-derived TGF-beta. *J Immunol* **178**: 2883–2892.

Loddenkemper C, Schernus M, Noutsias M, Stein H, Thiel E, Nagorsen D (2006) In situ analysis of FOXP3 + regulatory T cells in human colorectal cancer. *J Transl Med* **4**: 52.

Mansfield R, Able S, Griffin P, Irvine B, James I, Macartney M, Miller K, Mills J, Napier C, Navratilova I, Perros M, Rickett G, Root H, van der Ryst E, Westby M, Dorr P (2009) CCR5 pharmacology methodologies and associated applications. *Methods Enzymol* **460**: 17–55.

McMurchy AN, Levings MK (2012) Suppression assays with human T regulatory cells: A technical guide. *Eur J Immunol* **42**: 27–34.

Mizukami Y, Kono K, Kawaguchi Y, Akaike H, Kamimura K, Sugai H, Fujii H (2008) CCL17 and CCL22 chemokines within tumor microenvironment are related to accumulation of Foxp3 + regulatory T cells in gastric cancer. *Int J Cancer* **122**: 2286–2293.

Mueller A, Strange PG (2004) Mechanisms of internalization and recycling of the chemokine receptor, CCR5. *Eur J Biochem FEBS* **271**: 243–252.

Mulder WMC, Koenen H, Muysenberg AJC, Bloemena E, Wagsfaff J, Scheper RJ (1994) Reduced expression of distinct T-cell CD molecules by collagenase/DNase treatment. *Cancer Immunol Immunother* **38**: 253–258.

Ray N (2009) Maraviroc in the treatment of HIV infection. *Drug Des Devel Ther* **2**: 151–161.

Richardson MW, Jadlowsky J, Didigu CA, Doms RW, Riley JL (2012) KLF2 modulates CCR5 expression and susceptibility to HIV-1 infection. *J Immunol* **189**: 3815–3821.

Saita Y, Kondo M, Shimizu Y (2007) Species selectivity of small-molecular antagonists for the CCR5 chemokine receptor. *Int Immunopharmacol* **7**: 1528–1534.

Salama P, Phillips M, Grieu F, Morris M, Zeps N, Joseph D, Platell C, Iacopetta B (2009) Tumor-infiltrating FOXP3 + T regulatory cells show strong prognostic significance in colorectal cancer. *J Clin Oncol* **27**: 186–192.

Schlecker E, Stojanovic A, Eisen C, Quack C, Falk CS, Umansky V, Cerwenka A (2012) Tumor-infiltrating monocytic myeloid-derived suppressor cells mediate CCR5-dependent recruitment of regulatory T cells favoring tumor growth. *J Immunol* **189**: 5602–5611.

Sinicrope FA, Rego RL, Ansell SM, Knutson KL, Foster NR, Sargent DJ (2009) Intraepithelial effector (CD3 +)/regulatory (FoxP3 +) T-cell ratio predicts a clinical outcome of human colon carcinoma. *Gastroenterology* **137**: 1270–1279.

Song JK, Park MH, Choi D-Y, Yoo HS, Han SB, Yoon DY, Hong JT (2012) Deficiency of C-C chemokine receptor 5 suppresses tumor development via inactivation of NF-κB and upregulation of IL-1Ra in melanoma model. *PLoS One* **7**: e33747.

Spring H, Schüler T, Arnold B, Hämmerling GJ, Ganss R (2005) Chemokines direct endothelial progenitors into tumor neovessels. *Proc Natl Acad Sci USA* **102**: 18111–18116.

Tan MCB, Goedegebuure PS, Belt BA, Flaherty B, Sankpal N, Gillanders WE, Eberlein TJ, Hsieh C-S, Linehan DC (2009) Disruption of CCR5-dependent homing of regulatory T cells inhibits tumor growth in a murine model of pancreatic cancer. *J Immunol* **182**: 1746–1755.

Tatura R, Zeschnigk M, Adamzik M, Probst-Kepper M, Buer J, Kehrmann J (2012) Quantification of regulatory T cells in septic patients by real-time PCR-based methylation assay and flow cytometry. *PLoS One* **7**: e49962.

Terme M, Pernot S, Marcheteau E, Sandoval F, Benhamouda N, Colussi O, Dubreuil O, Carpentier AF, Tartour E, Taieb J (2013) VEGFA-VEGFR pathway blockade inhibits tumor-induced regulatory T-cell proliferation in colorectal cancer. *Cancer Res* **73**: 539–549.

Wainwright DA, Sengupta S, Han Y, Lesniak MS (2011) Thymus-derived rather than tumor-induced regulatory T cells predominate in brain tumors. *Neuro-Oncol* **13**: 1308–1323.

Wierda RJ, Kuipers HF, van Eggermond MCJA, Benard A, van Leeuwen JC, Carluccio S, Geutskens SB, Jukema JW, Marquez VE, Quax PHA, van den Elsen PJ (2012) Epigenetic control of CCR5 transcript levels in immune cells and modulation by small molecules inhibitors. *J Cell Mol Med* **16**: 1866–1877.

Yoon HH, Orrock JM, Foster NR, Sargent DJ, Smyrk TC, Sinicrope FA (2012) Prognostic impact of FoxP3 + regulatory T cells in relation to CD8 + T lymphocyte density in human colon carcinomas. *PloS One* **7**: e42274.

Supplementary Information accompanies this paper on British Journal of Cancer website (http://www.nature.com/bjc)